METHANE TO NITROGEN MIXING RATIO ACROSS THE SURFACE OF PLUTO. S. Protopapa[1], K.L. Berry[2], R.P. Binzel[3], J.C. Cook[4], D. P. Cruikshank[5], C.M. Dalle Ore[6,5], A.M. Earle[3], K. Ennico[5], W.M. Grundy[7], D.E. Jennings[8], C.J.A. Howett[4], I.R. Linscott[9], A.W. Lunsford[8], C.B. Olkin[4], A.H. Parker[4], J.Wm. Parker[4], S. Philippe[10], E. Quirico[10], D.C. Reuter[8], B. Schmitt[10], K.N. Singer[4], J.R. Spencer[4], J.A. Stansberry[11], S.A. Stern[4], C.C.C. Tsang[4], A.J. Verbiscer[12], H.A. Weaver[13], L.A. Young[4]. [1]University of Maryland (protopapa@astro.umd.edu), [2]Northern Arizona University and United States Geological Survey, [3]Massachusetts Institute of Technology, [4]Southwest Research Institute, [5]NASA Ames Research Center, [6]SETI Institute, [7]Lowell Observatory, [8]NASA Goddard Space Flight Center, [9]Stanford University, [10]Université Joseph Fourier, [11]Space Telescope Science Institute, [12]University of Virginia, [13]Johns Hopkins University Applied Physics Laboratory.

Introduction: NASA's *New Horizons* mission completed a close approach to the Pluto system on 14 July 2015 reaching a distance of 12,000 km from Pluto's surface [1]. *New Horizons* observations revealed Pluto's striking variations in the distribution of the volatile ices N_2, CH_4, and CO and non volatile H_2O ice [2]. These results rely on the analysis of spectral parameters, including band depth and equivalent width. However, the main limitation of such approach is the incapability of disentangling relative abundance from grain size effects. It is possible to overcome such limitation only by means of radiative transfer modeling of the absorption bands. We will discuss constraints on the abundances and scattering properties of the materials across the surface of Pluto, focusing mainly on the distribution of N_2 and CH_4 ices. These are among the volatiles that support Pluto's atmosphere and understanding their distribution and correlation with surface geology is vital to set observational constraints for volatile transport models [3].

Observations: Spatially resolved near-infrared spectra of Pluto's surface were acquired using the Linear Etalon Imaging Spectral Array (LEISA), part of the *New Horizons* Ralph instrument [4]. LEISA produces infrared spectra in the 1.25-2.5 μm and 2.1-2.25 μm spectral range at the resolving power ($\lambda/\Delta\lambda$) of 240 and 560, respectively. The 1.25-2.5 μm segment is used to infer the surface composition of Pluto as outer solar system ices such as N_2, CH_4, H_2O have strong unique absorption bands in this wavelength region. The 2.1-2.25 μm segment is instead sensitive to the spectral shape of the 2.15-μm absorption band of N_2 ice, which is temperature dependent. A number of LEISA observations have been downloaded to Earth. In this paper we present two LEISA resolved scans of Pluto collected at a distance from Pluto's center of ~100,000 km at a spatial resolution of 6 and 7 km/pixel. The two scans combined cover Pluto's full disk.

Spectral Modeling: The quantitative analysis of Pluto's spectra is performed using the Hapke radiative transfer model [5]. Specifically, the bidirectional reflectance of a geographical or an intimate mixture is computed. The input parameters are the optical constants of the surface ices in the mixture together with the viewing geometry. The free parameters in the model are grain size and contribution of each surface terrain to the mixture, together with cosine asymmetry parameter, compaction parameter and mean roughness slope which are related to anisotropic scattering, opposition effect and large-scale roughness, respectively. They are iteratively modified by means of a chi-squared minimization algorithm until a best fit to the observations is obtained. To determine a spatial map for each of the physical quantites in the model (*e.g.*, abundance and grain size of each surface material) a parallel-computing, pixel-by-pixel, modeling analysis is performed. This approach requires the application of the same modeling strategy across all surface at the expense of possible compositional peculiarities across small surface areas.

Results: The pixel-by-pixel modeling analysis is applied to the LEISA data degraded to a spatial resolution of ~40 km/pixel, as this approach is highly computationally expensive. An areal mixture of H_2O ice, Titan tholin, methane saturated with nitrogen (CH_4:N_2) and nitrogen saturated with methane (N_2:CH_4) provides a reasonable fit to all Pluto spectra. The abundance maps obtained from the pixel-by-pixel modeling analysis for H_2O ice, CH_4:N_2 and N_2:CH_4 are combined in a false color image shown in Fig. 1. Note that the green coloring of the south east limb is an artificat. The comparison between the spectra extracted in regions of interest and the modeling is shown in Fig. 2. The results presented in this abstract are preliminary and as obvious from Fig. 2 there is still margin for improvement in the modeling. However, as mentioned above, this is an automated process and a perfect match between observations and model is beyond the scope of the analysis. The results obtained rely on the choice of the surface materials and set of optical constants. To give an example, Titan tholin is used in this analysis as color agent to decrease the albedo levels in regions as Cthulhu Regio[1] or Baré Montes. However, there are

[1]All place names mentioned in this abstract are informal.

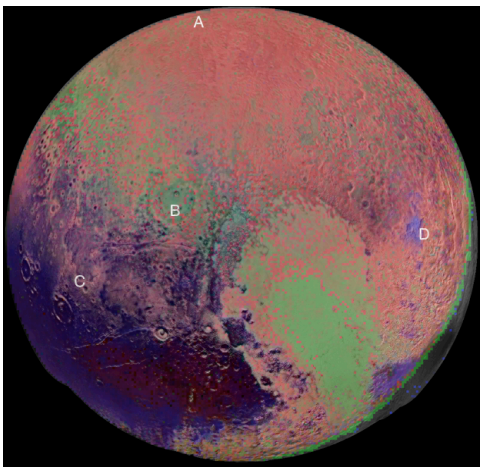

Fig. 1: False color image obtained combining the abundance maps of CH_4:N_2 (red), N_2:CH_4 (green), and H_2O ice (blue) obtained from the pixel-by pixel modeling analysis. A-D label regions of interest whose spectra are displayed in Fig. 2 color-coded as in the map.

several kinds of tholins [6] and the search for the most appropriate one was not the goal of this preliminary study. Keeping this in mind, we anticipate that the highest tholin concentration occurs in the dark reddish terrains revealed by the Ralph/MVIC color images [1,4], as expected. Regions with the highest concentration of H_2O ice (above ~30%) agree with those highlighted by the correlation method between each Pluto's spectrum and the model spectrum of crystalline H_2O ice [2]. However, the modeling analysis reveals a more widespread distribution of this non volatile component which extends to areas such as Piri Rupes and Bird Planitia. A detailed analysis of the H_2O ice spatial distribution is given by [7]. The use of the two phases CH_4:N_2 and N_2:CH_4 is dictated by thermodynamic equilibrium [8]. For the time being we approximate CH_4:N_2 by pure CH_4 and obtain the optical constants for N_2:CH_4 as described by [9]. An abundance of one of the two phases equal to zero would imply that thermodynamic equilibrium does no longer apply. The CH_4-dominated component is widespread across Pluto surface (red color in Fig. 1). The N_2-enrich component dominates in Sputnik Planum and in many craters floors like Burney. For a plausible Pluto surface temperature of 40 K, the N_2-CH_4 binary phase diagram shows that, in the case of thermodynamic equilibrium, the solubility limit of CH_4 in N_2 is about 5%. However, setting this as a constraint failed to reproduce the strong 2.15-µm N_2 band common to areas in green in Fig. 1. A representative spectrum is shown in Fig. 2, panel B. Notice that such absorption band is less prominent to absent in spectra extracted for example in the northern polar region (spectrum A in Fig. 2). If we let the concentration of CH_4 in N_2 vary, we find that amounts less than 5% are needed to reproduce the 2.15-µm band. If we interpret this finding in terms of thermodynamic equilibrium, since we do not get a null contribution of the CH_4:N_2 component, this would imply a much lower temperature in regions like Sputnik Planum. The temperature interpretation will be further investigated by the analysis of the 2.1-2.25 µm LEISA segment and exploration of different modeling approaches.

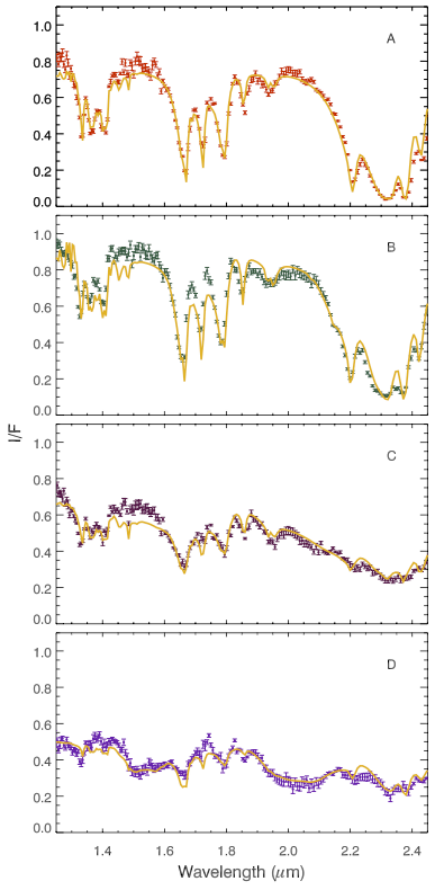

Fig. 2: Spectra corresponding to the regions of interest labeled in Fig. 1 and characterized by different composition are displayed. The observations are compared to the best-fit models shown in gold solid line.

References: [1] Stern S. A. et al. (2015) *Science, 350,* aad1815. [2] Grundy W. M. et al. (2016) *Science*, submitted. [3] Young L. A. (2013) *The Astrophysical Journal Letters, 766,* L22. [4] Reuter D. C. et al. (2008) *Space Science Reviews, 140,* 129. [5] Hapke B. (1993) *Topics in Remote Sensing, vol. 3,* Cambridge, UK: Cambridge University Press. [6] Cruikshank D. P. (2016) *LPSC 47*. [7] Cook J. C. (2016) *LPSC 47*. [8] Protopapa S. et al. (2015) *Icarus, 253*, 179. [9] Douté S. et al. (1999), *Icarus, 142*, 421.